International Journal of Environmental Sciences
ISSN: 2229-7359
Vol. 11 No. 5,2025
https://theaspd.com/index.php

Model-Based Evaluation of Li–NCM Battery Performance for Environmentally Resilient Energy Systems

Prabhu S[1],Vinod S[2],Rudhra S[3], Balaji M[4],
[1] Department of Electrical and Electronics Engineering, Mohan babu University, A. Rangampeta, Tirupati 517102, Andhra Pradesh, India.
[2,3] Department of Electrical and Electronics Engineering, Jerusalem College of Engineering, Anna University, Chennai 600100, Tamil Nadu, India.
[4] Department of Electrical and Electronics Engineering, Sri Sivasubramaniya Nadar College of Engineering, Kalavakkam 603110, Tamil Nadu, India
prabhutajmahal6@gmail.com[1],vinod@jerusalemengg.ac.in[2],rudhra@jerusalemengg.ac.in[3],
balajim@ssn.edu.in[4],

Abstract *This research is to thoroughly investigate the design and operational behaviour of lithium-ion cells that utilize Nickel Cobalt Manganese (Li–NCM) as the cathode material. These types of batteries are widely used in electric vehicles (EVs) and stationary energy systems, where consistent performance, thermal stability, and energy efficiency are critical. To meet the growing demand for safer and more sustainable energy storage, this study adopts a detailed, simulation-based approach to optimize and evaluate cell performance under practical cycling conditions. Using Battery Design Studio as the modelling platform, the study begins with a structured design of the battery cell, including the selection and specification of electrode geometry, electrolyte blends, separator characteristics, and packaging configuration. The model integrates both electrical (RCRTable3D equivalent-circuit) and thermal domains to capture the cell's response during typical charge–discharge cycles. These simulations are carried out at a controlled ambient temperature of 25 °C, with forced convection cooling set at 100 W/m²·K to mimic field-like thermal behaviour. Special attention is given to the materials used in the construction of the cell—such as NCM cathodes, graphite anodes, custom electrolyte formulations, and layered casings—to examine how each element influences overall cell behaviour. Key performance metrics, including voltage consistency, temperature rise, capacity retention, and energy output, are analysed. The ultimate objective is to derive insights that contribute to more robust, efficient, and environmentally sound battery systems suitable for future energy and mobility applications.*

Keywords: *Lithium-ion battery, Li–NCM cathode, Battery Design Studio, Thermal analysis, Energy storage systems.*

INTRODUCTION

Lithium Nickel Cobalt Manganese Oxide (Li-NCM) batteries are highly regarded for their superior energy density, long cycle life, and stable electrochemical behaviour. These characteristics make them a popular choice in electric vehicles (EVs), grid-scale energy storage systems, and portable electronic devices [1,2]. The chemistry of Li-NCM cells strikes a balance—nickel contributes high capacity, cobalt enhances structural stability, and manganese improves safety—resulting in efficient power delivery and extended durability [3,4]. Despite their advantages, the real-world performance of Li-NCM batteries is influenced by several critical factors, including thermal stability, voltage characteristics, capacity retention, and overall energy efficiency [5,6]. Among these, thermal stability remains a key concern. Heat generation caused by internal resistance or high current loads can degrade performance and, in severe cases, lead to thermal runaway [7,8]. Ensuring safe operation under these conditions requires effective thermal management strategies [9]. Equally important is monitoring the State of Charge (SOC), which offers insights into how effectively the battery stores and delivers energy throughout its cycling life [10,11]. Voltage behaviour during charge and discharge cycles helps evaluate internal resistance and detect early signs of degradation or polarization [12]. Additionally, capacity retention over time reflects how well the battery maintains its ability to hold a charge, often affected by electrode wear and side reactions [13]. Advanced diagnostic tools, such as differential capacity (dQ/dV) analysis, are essential for tracking aging behaviour and optimizing charge management protocols [14,15]. This study aims to provide a detailed evaluation of Li-NCM battery performance, supporting efforts to improve design, extend lifespan, and enhance the reliability of next-generation energy systems.

LITERATURE REVIEW

.Britala et al. (2023) presented a detailed review of degradation mechanisms affecting NCM cathodes, emphasizing factors like structural instability, side reactions at the electrolyte interface, and phase transformations during deep cycling. Their work underscores the necessity of optimizing cell chemistry and thermal control to extend cycle life in practical applications.

In their study, Brosa Planella et al. (2022) provided a comprehensive classification of physics-based battery models, including electrochemical, thermal, and equivalent-circuit approaches. They highlighted the growing importance of coupled modeling frameworks for understanding multi-domain interactions within Li-ion cells, especially under dynamic loads.

Ramadass et al. (2003) developed one of the earliest predictive models for capacity fade in lithium-ion batteries, correlating it with structural aging and the growth of the solid electrolyte interphase (SEI). Their findings laid the groundwork for modern simulation tools that estimate long-term battery performance based on cycling behavior.

Steinhardt et al. (2023) examined how equivalent circuit model (ECM) parameters affect thermal prediction in real-life drive cycles. Their work highlighted the sensitivity of heat generation estimates to parameter variability, advocating for real-time model calibration in battery management systems.

Lin et al. (2019) provided an overview of advanced battery modelling and state estimation techniques. They proposed integrating data-driven algorithms with physics-based models to improve accuracy in predicting internal states like state of charge (SOC) and temperature both vital for safe and efficient battery operation.

DESIGNING OF LI-NCM BATTERY CELL

3.1 Battery Design and Simulation Workflow

The systematic approach for designing a battery using Battery Design Studio. The process begins with launching the software and creating a new workspace. The user then selects the preferred cell type, such as a Li-NCM Standard cell in cylindrical, pouch, or prismatic form. Next, the cell structure is defined by specifying electrode properties, configuring the separator, setting electrolyte characteristics, selecting packaging options, and adjusting internal components. Following this, model configurations are established, including electrolyte parameter settings, defining IET models, and optionally integrating thermal models. After completing the setup, the user inputs simulation parameters and runs the simulations[15,16]. The generated results are analysed through graphical representations, providing a comprehensive evaluation of the battery's performance. Finally, the findings are reviewed, and the results are saved for future reference or further optimization.

3.2Battery Design and Component Selection

Lithium-ion batteries utilizing Li-NCM Standard chemistry are a preferred choice for electric vehicles (EVs) due to their superior energy density, efficiency, and thermal stability. The battery design process involves selecting high-performance materials for its essential components, including the cathode, anode, electrolyte, separator, and casing. The cathode, composed of lithium nickel cobalt manganese oxide (Li-NCM), offers an excellent balance of energy capacity, cycle longevity, and thermal safety. The anode, typically made of graphite, ensures stable charge storage and enhances long-term battery performance. The electrolyte consists of lithium salts dissolved in organic solvents, enabling smooth ion transport and optimizing charge- discharge efficiency [17,18,19]. A polymer separator is incorporated to prevent short circuits while allowing controlled ion flow between the electrodes. To ensure mechanical protection and structural integrity, the battery casing is made from durable materials like aluminum or stainless steel[20, 21,22]. Effective thermal management strategies, such as liquid cooling systems, heat-dissipating materials, or phase change components, are integrated to regulate temperature and enhance battery lifespan. Each component is carefully chosen and engineered to improve safety, energy efficiency, and durability, making Li-NCM Standard prismatic cells highly suitable for EV applications. Their advanced design not only supports high-performance energy storage but also contributes to the reliability and sustainability of modern electric mobility solutions which is shown in figure 3.1. By optimizing material selection and thermal control, these batteries help maximize performance, reduce energy

losses, and extend operational lifespan, ensuring they meet the growing demands of next-generation transportation systems.

The coated foil electrode is a key component in prismatic lithium-ion batteries, enabling efficient energy transfer during charge and discharge cycles. It consists of a thin metal foil that acts as a current collector—aluminum for the cathode (positive electrode) and copper for the anode (negative electrode) [23,24]. A specialized active material layer is applied to the surface of each foil to enhance electrochemical performance. The cathode is coated with Lithium Nickel Cobalt Manganese Oxide (Li-NCM) Standard Chemistry, which is valued for its high energy density, stability, and long cycle life. On the other hand, the anode is coated with graphite or silicon- based materials to improve lithium-ion storage capacity and electrical conductivity. These coatings play a crucial role in facilitating ion exchange during battery operation, ensuring efficient energy conversion, stable performance, and extended battery lifespan [25,26]. By optimizing material composition and layer uniformity, the coated foil electrodes contribute to improved energy efficiency, making them ideal for demanding applications such as electric vehicles and energy storage systems.

$$Li_xC + M \rightarrow C + Li_xM$$

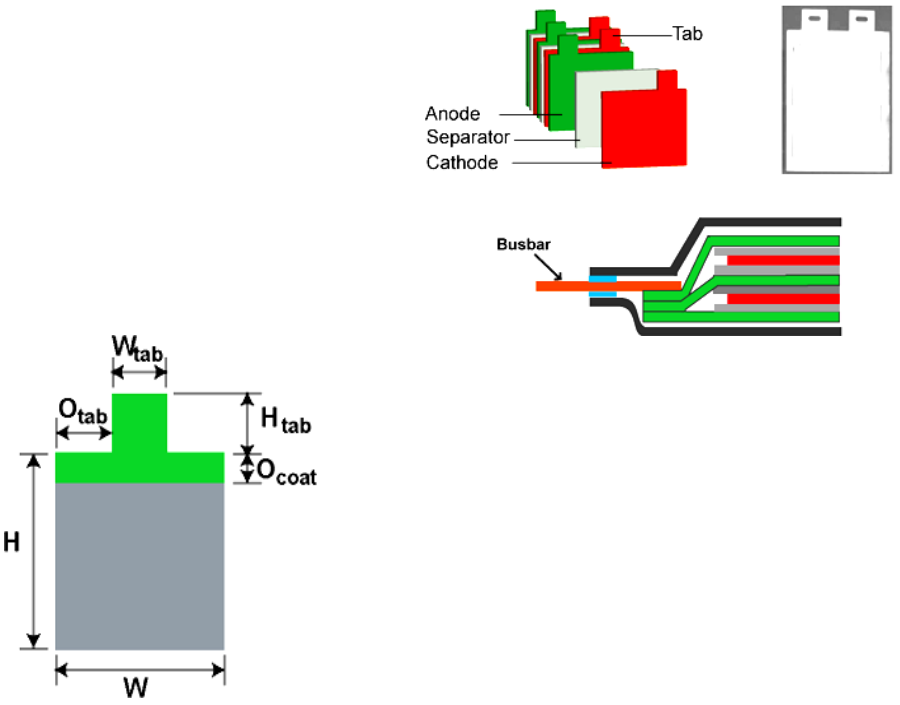

Figure. 3.2: Layout of the coated foil electrode with a single sided tab for Li-NCM Cell electrodes.

Each electrode is equipped with a single-sided tab that serves as an electrical connection to the external circuit. This tab, made from the same metal as the electrode foil, extends from one side to ensure efficient current collection[27,28,29]. To maintain a secure and reliable connection, a designated portion of the foil near the tab remains uncoated (O coat), preventing interference from the active material. The tab's dimensions, including its width (W tab) and height (H tab), are precisely engineered to enhance electrical conductivity while minimizing resistance. Proper alignment of the positive and negative electrodes plays a crucial role in optimizing battery efficiency, improving energy density, and maintaining stable thermal performance. By strategically designing tab placement and refining the coating process is shown in figure 3.2, manufacturers can enhance the battery's overall durability, safety, and long-term operational stability. These improvements make prismatic lithium-ion cells highly suitable for high- performance applications, including electric vehicles and large-scale energy storage systems.

Parameter	Value		
Height (h), mm	149.000	Tab width (wtab), mm	35.000
Width (w), mm	86.000	Tab height (htab), mm	20.000
Tab offset (Otab)	3.000	Coat. offset (Ocoat), mm	0.000

Fig. 3.3: Dimensions of the coated foil electrode with a single sided tab for positive and negative electrodes for Li-NCM Cell.

Figure 3.3 presents the dimensions of a coated foil electrode featuring a single-sided tab configuration for both positive and negative terminals. It outlines essential parameters such as electrode width, tab length, tape width, and spacing, ensuring precise alignment and material consistency. This structured design enhances electrical conductivity, facilitates uniform coating application, and contributes to the overall efficiency and performance of the battery by minimizing resistance and optimizing current flow.

3.3Electrode Materials and Properties

TABLE III.I ELECTRODE MATERIALS & PROPERTIES OF LI-NCM CELL

Material Type	Positive Electrode Material	Positive Weight Fraction	Positive Volume Fraction	Positive Density (g/cm^3)	Negative Electrode Material	Negative Weight Fraction	Negative Volume Fraction	Negative Density (g/cm^3)
Active Material	NCM	0.980	0.948	4.740	Graphitefade	0.980	0.975	2.230
Binder	PVDF	0.020	0.052	1.770	PVDF	0.020	0.025	1.770
Conductivity Aid	Carbon Black	0.000	0.000	1.950	Carbon Black	0.000	0.000	1.950
Total	-	1.000	1.000	4.586	-	1.000	1.000	2.218

able III.I provides a detailed composition of the electrode materials used in a lithium-ion battery, outlining their weight fraction, volume fraction, and density. The positive electrode (cathode) consists primarily of Nickel Cobalt Manganese Oxide (NCM), which makes up 98.0% by weight and 94.8% by volume, offering high energy density and stability with a density of 4.740 g/cm³. It is bound by 2.0% Polyvinylidene Fluoride (PVDF), ensuring structural integrity, while Carbon Black, present in negligible amounts, enhances conductivity[30,31,32]. Similarly, the negative electrode (anode) is composed of 98.0% graphite, enabling efficient lithium-ion storage with a density of 2.230 g/cm³. PVDF, at 2.0% weight and 2.5% volume, binds the structure, while Carbon Black's minimal presence emphasizes reliance on graphite for conductivity. The overall density of the cathode (4.586 g/cm³) is higher than that of the anode (2.218 g/cm³), indicating greater mass contribution from NCM. This composition ensures an optimal balance between energy storage, conductivity, and structural stability, making the battery highly efficient and durable for applications such as electric vehicles and energy storage systems.

3.4 Separator and Electrolyte Specifications

The polypropylene separator serves as a crucial barrier between electrodes in lithium-ion batteries, preventing electrical short circuits while allowing smooth ion flow. Its strong durability, excellent thermal stability, and high chemical resistance contribute to enhanced battery safety and overall efficiency. By maintaining separation and supporting electrochemical processes, this component plays a key role in extending battery lifespan and ensuring reliable performance in energy storage and electric vehicle applications.

TABLE III.II : ELECTROLYTE SPECIFICATIONS OF LI-NCM CELL

Sl.no	Type	Name	Solvent Weight Fraction	Solvent Volume Fraction	Molality (mol/kg solvent)	Solvent Density (g/cm³)	Weight Fraction	Volume Fraction
1	Solvent	DMC - Dimethyl Carbonate	0.333	0.347	-	1.069	0.288	0.311
2	Salt	$LiPF_6$ - Lithium Hexafluorophosphate	-	-	1.027	-	0.135	0.104
3	Solvent	Ethyl Methyl Carbonate	0.333	0.371	-	1.000	0.288	0.333
4	Solvent	EC - Ethylene Carbonate	0.333	0.281	-	1.321	0.288	0.252
Total	-	-	1.000	1.000	1.027	1.114	-	-

Table III.II presents the electrolyte composition and properties in lithium-ion batteries, highlighting the role of solvents and lithium salt. It consists of Dimethyl Carbonate (DMC), Ethyl Methyl Carbonate (EMC), and Ethylene Carbonate (EC), each with an equal weight fraction of 0.333, ensuring efficient ion transport. Their densities—1.069 g/cm³ (DMC), 1.000 g/cm³ (EMC), and 1.321 g/cm³ (EC)—affect viscosity and conductivity. Lithium Hexafluorophosphate ($LiPF_6$), with a molality of 1.027 mol/kg solvent, supports ion movement. The electrolyte density is 1.114 g/cm³, with an average material cost of $13.18/kg, balancing performance, stability, and affordability.

3.5 Packaging Type and Design Considerations

The Packaging Type and Design Considerations focus on the materials used in battery enclosures, specifying their thickness, density, and functional purpose. The structure comprises three layers: nylon (40 µm, 1.40 g/cm³) for mechanical reinforcement, aluminum (1100) (40 µm, 2.70 g/cm³) to shield against moisture and contaminants, and polypropylene (40 µm, 0.90 g/cm³) for insulation and chemical stability. This multi-layered construction improves durability, safety, and thermal resistance, ensuring long-term battery reliability.

3.6 Cell Voltage limits and State-of-Charge (SOC) Settings:

TABLE III.III : CELL VOLTAGE LIMITS AND SOC SETTINGS OF LI-NCM CELL.

Category	Parameter	Value
Stoichiometry at Formation	Negative	0.200
	Positive	0.490
Voltage Limits	Lower (min = 2.63V)	2.63
	Upper (max = 5.97V)	3.60
	Positive Average	3.84
	Negative Average	0.61
	Cell Average	3.24
Cell State	Cell Equilibrium Voltage (V)	3.60
	SOC (%)	100.00
Stoichiometry	Positive Stoichiometry	0.579 - 0.629
	Negative Stoichiometry	0.00029 - 0.073

Table III.III presents the voltage limits and state-of-charge (SOC) settings for the lithium- ion cell, outlining critical parameters for optimal performance. The stoichiometry at formation is 0.200 for the negative electrode and 0.490 for the positive electrode, indicating initial lithium content distribution. Voltage constraints include a minimum of 2.63V and a maximum of 3.60V, ensuring safe operation. The average voltages recorded are 3.84V for the positive electrode, 0.61V for the negative electrode, and 3.24V for the overall cell. At equilibrium, the cell maintains a voltage of 3.60V with a fully charged SOC of 100%. Additionally, the

stoichiometry range varies between 0.579 - 0.629 for the positive electrode and 0.00029 - 0.073 for the negative electrode, reflecting lithium intercalation levels. These values help define the battery's charge-discharge characteristics and operational efficiency.

LI-NCM STANDARD Cell Report

TABLE III.IV: CELL PROPERTIES

Cell Properties	Value
State of Charge (%)	100.00
Voltage (V)	3.24
Capacity (Ahr)	0.89
Energy (Whr)	2.881
Energy Density	
Whr/kg	16.837
Whr/liter	32.603
Weight (g)	171.104
Volume (cm^3)	88.362
Materials Cost ($)	4.38
Active Area (m^2)	0.154
Unit Capacity (mAh/cm^2)	1.599
C/A Ratio (mAh/mAh)	1.436
Electrolyte Mass (g)	41.387
Electrolyte Volume (cm^3)	35.855
Separator Area (m^2)	0.165
Heat Capacity @25°C (J/g-K)	0.868
Cell Dimensions	
Length (mm)	190.000
Breadth (mm)	100.000
Thickness (mm)	6.360

This table III.IV outlines the fundamental characteristics of the lithium-ion cell, focusing on its energy storage capacity, dimensions, and material costs. Operating at a full state of charge (100%), the cell has a voltage of 3.24V and a capacity of 0.89 Ah, yielding an energy output of 2.881 Wh. It maintains an energy density of 16.837 Wh/kg and 32.603 Wh/liter, ensuring high power efficiency. Weighing 171.104 g with a volume of 88.362 cm^3, it remains lightweight and compact. The electrolyte properties, including a mass of 41.387 g and a volume of 35.855 cm^3, contribute to stable ion transport. The separator area is 0.165 m^2, providing adequate insulation between electrodes. With a heat capacity of 0.868 J/g-K at 25°C, the cell is designed to manage thermal conditions efficiently. Its structural dimensions—190 mm in length, 100 mm in breadth, and 6.36 mm in thickness—make it suitable for various applications, ensuring reliability and performance.

TABLE III.V : STACK PROPERTIES OF LI-NCM CELL

Stack Properties	Value
Energy Density	
Whr/kg	22.524
Whr/liter	34.186
Weight (g)	127.906
Volume (cm^3)	84.272

Height (mm)	153.000
Width (mm)	90.000
Thickness (mm)	6.120

The stack properties define the battery's overall performance when multiple cells are combined. It achieves an energy density of 22.524 Wh/kg and 34.186 Wh/liter, surpassing that of a single cell, making it suitable for high-energy applications. The total weight of the stack is 127.906 g, with a volume of 84.272 cm^3, ensuring compact and lightweight energy storage. Its dimensions—153 mm in height, 90 mm in width, and 6.12 mm in thickness—highlight its optimized design for efficient packaging. The balance between energy density and volume utilization makes the stack configuration ideal for electric vehicle batteries and large-scale energy storage systems, maximizing both performance and space efficiency.

TABLE III.VI : COMPUTED ELECTRODE PROPERTIES VALUES OF LI-NCM CELL

Computed Electrode Properties	Positive Value	Negative Value
Average Voltage (V)	3.84	0.61
Stoichiometry at Formation	0.490	0.200
Unit Capacity (mAh/cm^2)	5.858	1.599
Thickness (w/ collector) (µm)	320.000	300.000
Coating Porosity (%)	33.8	30.5
Coated Area (cm^2)	128.140	132.880
Coating Thickness (µm)	150.000	145.000
Coating Weight (g)	5.835	2.971
Loading (mg/cm^2)	45.536	22.355

The table III.VI details the key properties of the electrodes, which influence the overall efficiency and stability of the battery. The positive electrode operates at an average voltage of 3.84V, while the negative electrode functions at 0.61V, ensuring a stable charge-discharge cycle. Stoichiometry values at formation are 0.490 for the positive electrode and 0.200 for the negative, indicating the material balance required for optimal performance. The unit capacity is 5.858 mAh/cm^2 for the positive electrode and 1.599 mAh/cm^2 for the negative. Electrode thickness, including the collector, is 320 µm for the positive and 300 µm for the negative. The porosity of the coating is 33.8% for the positive and 30.5% for the negative, allowing effective lithium-ion diffusion. The coated area is slightly larger for the negative electrode at 132.880 cm^2 compared to 128.140 cm^2 for the positive electrode. Coating thickness measures 150 µm for the positive and 145 µm for the negative, while the corresponding coating weights are 5.835 g and 2.971 g, respectively. Material loading per unit area is 45.536 mg/cm^2 for the positive and 22.355 mg/cm^2 for the negative, ensuring balanced electrochemical performance. These electrode parameters collectively contribute to the battery's energy storage capacity, cycle life, and operational efficiency.

4.Simulation and Performance Analysis

4.1 Procedure and cycler condition:

The given flowchart in figure 4.1 represents a structured charge-discharge cycle used for battery testing and performance evaluation. The Li-NCM Standard battery simulation setup follows a structured process to test charge-discharge characteristics. It begins with a 1A discharge until the voltage drops to 2.63V, followed by a 10-minute rest period to stabilize. The cell is then charged at 1A until it reaches 3.60V, ensuring proper energy storage. Another 10-minute rest follows to allow internal equilibrium. The cycle concludes with a final discharge at 1A down to 2.63V before ending. The setup maintains a constant ambient temperature of 25°C under forced convection with a heat transfer coefficient of 100 W/m^2-K, ensuring controlled thermal conditions for accurate battery performance analysis.

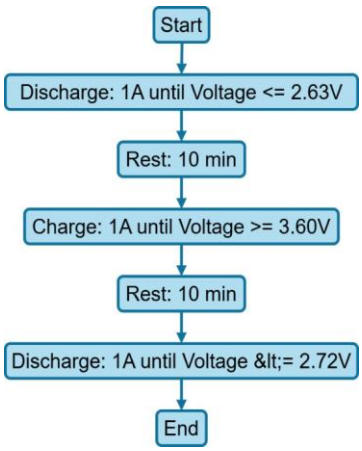

Figure. 4.1: Simulation of Designed battery with Charge-Discharge Cycler conditions for Li- NCM Cell

4.2Thermal Stability Analysis:

4.2.1Temperature vs. Time (Test (hr)):

The temperature increases gradually from 25.00°C to 25.03°C, indicating internal heating within the cell which is shown in figure.4.2. This steady rise in temperature suggests that the cell has a manageable thermal profile, with no abrupt surges. However, maintaining temperatures below 50°C is critical to preventing any detrimental effects on cell components. An efficient cooling system must be in place to manage temperature increases during heavy load conditions and avoid potential risks such as thermal runaway or degradation of materials.

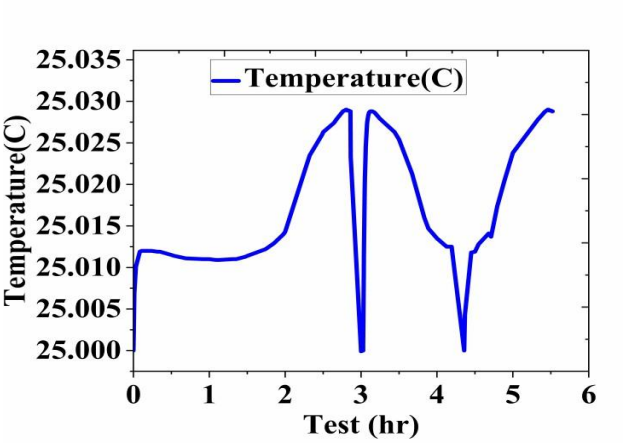

Figure. 4.2: Li-NCM Cell Temperature Profile of the Battery Over Time

4.2.2 Heat Generation vs. Time (Test (hr)): The heat generation fluctuates between 0.00000 W and 0.09110 W, with spikes occurring during high current periods which is shown in figure.4.3. These fluctuations are

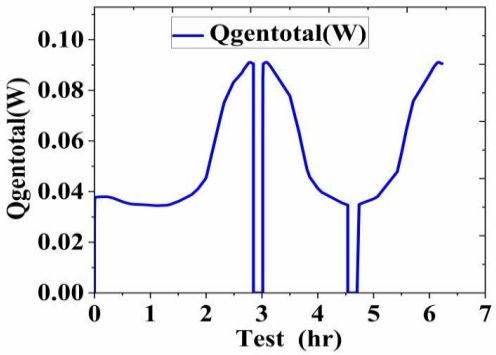

mainly caused by internal resistance and energy losses within the cell.

Figure. 4.3: Li-NCM Cell Heat Generation in the Battery System Over Time

International Journal of Environmental Sciences
ISSN: 2229-7359
Vol. 11 No. 5,2025
https://theaspd.com/index.php

The peaks in heat generation indicate that, while the cell is operating efficiently, higher power demands may result in inefficiencies. To prevent long-term performance degradation, it is essential to optimize current profiles and improve thermal management strategies to ensure the cell operates within safe thermal limits

4.2.3 Heat Balance vs. Time (Test (hr))

The heat balance consistently remains close to zero, indicating that the heat produced is being effectively dissipated. Minor fluctuations of around ±0.00231 W suggest that there are

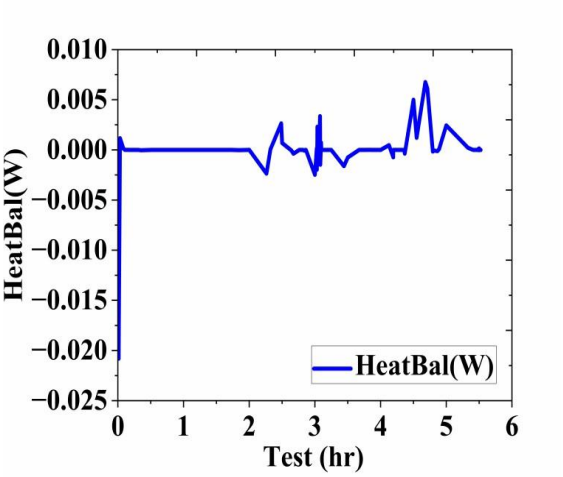

Figure. 4.4: Li-NCM Cell Heat Balance Distribution Throughout the Testing Period

slight inefficiencies in heat dissipation, but nothing that poses an immediate threat. If these variations increase, it could signal poor thermal management, leading to excess heat accumulation illustrated in figure 4.4. This, in turn, could degrade the cell's performance and reduce its lifespan. Continuous monitoring and optimization of thermal management systems are essential for maintaining long-term cell stability.

State of Charge (SOC) and Energy Efficiency

4.3.1SOC vs. Time (Test (hr)):

The SOC decreases smoothly from 99.99% to 1.37% throughout the discharge cycle, indicating that the cell is efficiently utilizing its stored energy. The gradual decline in SOC is evidence of controlled discharge with minimal fluctuations, suggesting low internal resistance and a steady current draw is illustrated in figure 4.5. This behavior ensures that the cell provides predictable performance without experiencing sudden drops in SOC or charge retention issues. It confirms that the cell is operating efficiently under the given conditions.

Figure. 4.5: Li-NCM Cell State of Charge (SOC) Profile Over Time

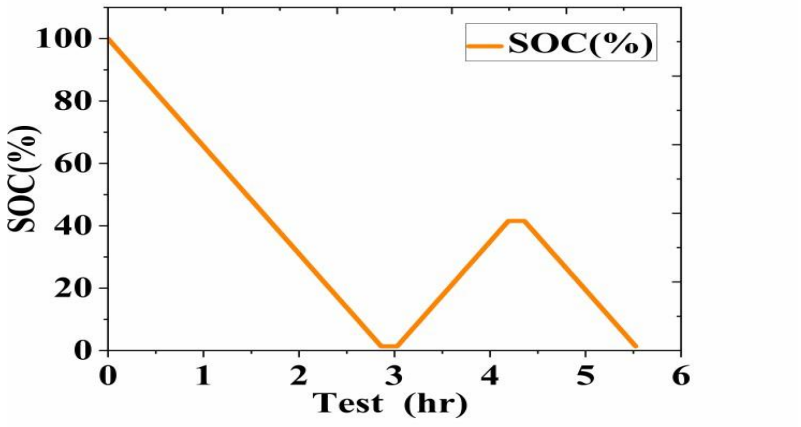

4.3.2 Cumulative Capacity and Energy vs. Time (Test (hr)):

The graph shown in figure. 4.6 presents cumulative capacity variation over time. Cumulative capacity increases steadily from 0.00000 Ah to 2.86011 Ah, reflecting efficient energy storage and delivery. The steady rise in cumulative capacity shows that the cell is making optimal use of its charge capacity with no apparent capacity fade or significant degradation. This consistent performance suggests that the electrodes are functioning effectively, and the cell is performing well.

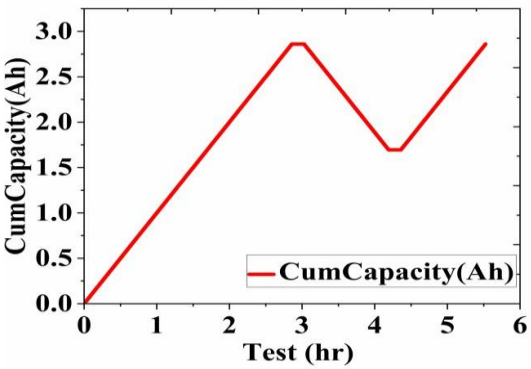

Figure. 4.6: Li-NCM Cell Cumulative Capacity Throughput Over Time

The absence of sudden drops in capacity supports the conclusion of stable, reliable performance over the testing period.

4.4Thermal and Electrical Properties:

4.4.1Thermal Conductivity and Heat Transfer vs. Time (Test (hr)):

Figure 4.7 illustrates a steady heat transfer coefficient in W/m²-K throughout the test period.

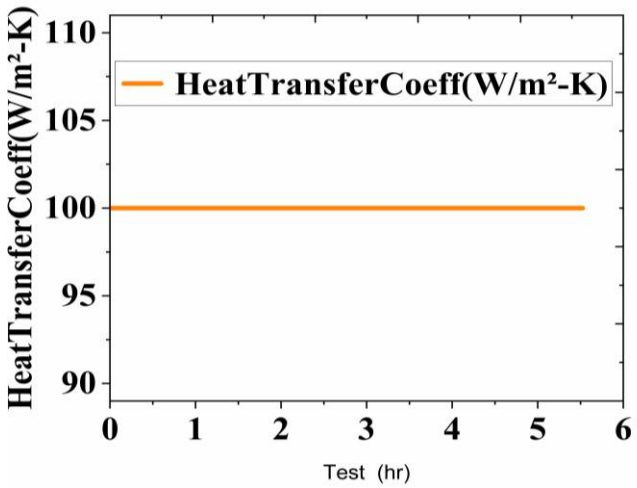

Figure4.7: Li-NCM Cell Heat transfer coefficient(W/m2-K) over Test Duration

The heat transfer coefficient remains stable at 100 W/m²-K, confirming that the cell is effectively dissipating heat. A stable coefficient indicates that the cell's thermal design is functioning as intended, ensuring that temperature remains within safe operational limits. If the heat transfer coefficient were to drop significantly below 80 W/m²-K, it could indicate insulation issues or resistance to heat flow, which could lead to overheating. This steady trend highlights the importance of proper thermal management to maintain cell stability and prevent thermal degradation.

4.4.2 Ohmic Resistance vs. Time (Test (hr)):

The ohmic resistance increases slightly from 0.00439 Ω·m² to 0.00459 Ω·m², which is a normal aging effect. This small increase is attributed to factors such as SEI layer growth and electrode material degradation over time is shown in figure.4.8. While this increase is expected, if the resistance exceeds 0.0045 Ω·m², it could signal more severe degradation or delamination of the electrodes. Monitoring resistance trends helps

predict aging and allows for adjustments in operational conditions or charging protocols to maintain optimal performance.

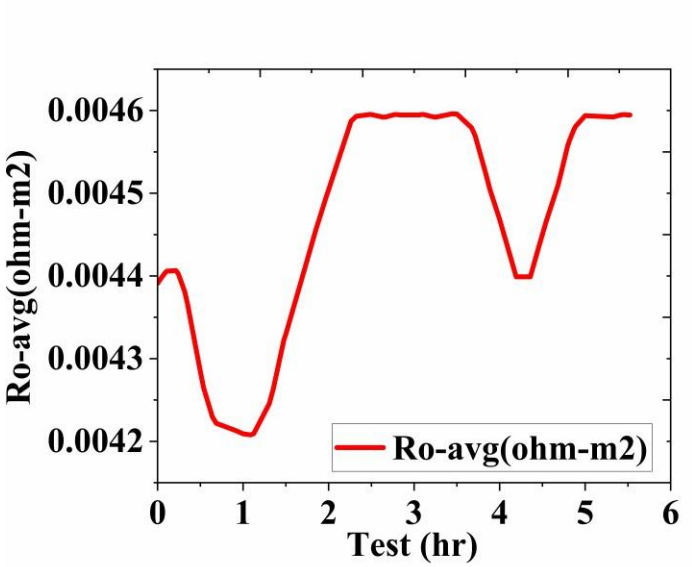

Figure 4.8: Li-NCM Cell Average Ohmic Resistance (ohm-m²) over Test Duration

4.4.3 Power Output vs. Time(hr):

The graph reveals a dynamic power profile with distinct fluctuations. Power output remains consistent, fluctuating between -3.60 W and 4.20 W, indicating that the cell is effectively delivering power under various load conditions. This stable output reflects efficient energy conversion and minimal impedance losses. If the power output were to fall below 3.8 W, it could suggest rising impedance or deteriorating internal conditions is shown in figure.4.9. Maintaining stable power output is crucial for ensuring the cell meets performance demands, particularly for applications that require continuous and reliable power delivery without significant degradation over time.

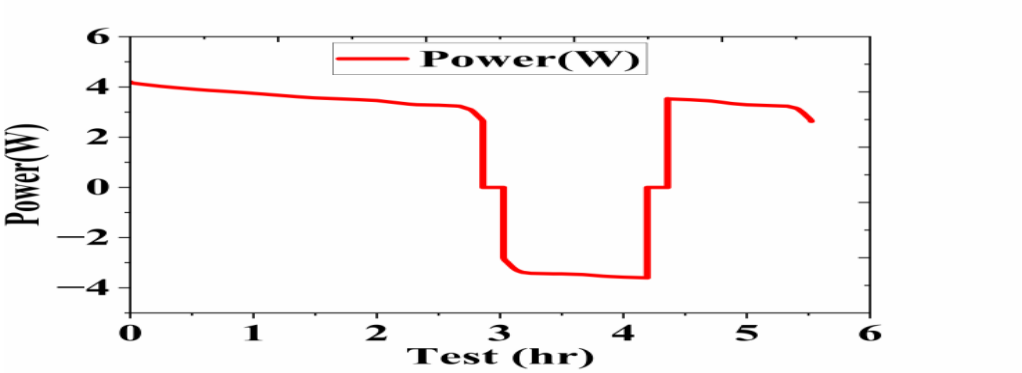

Figure. 4.9: Li-NCM Cell Power (W) over Test Duration

4.5Peak Analysis in dQ/dV for Li-NCM Standard Cell Aging

4.5.1Analysis of Differential Capacity vs. Voltage (Volts):

This graph shown in figure. 4.10 depicts the differential capacity (dQ/dV) of a cell as a function of voltage. The dQ/dV vs. Voltage graph provides crucial insights into the electrochemical behavior of the Li- NCM standard cell, highlighting lithium-ion intercalation and deintercalation processes during charge and discharge cycles. The most prominent peak appears at 2.660V with a dQ/dV value of 480.81 C/V, indicating a key phase transition. Additional peaks occur at 2.634V (-2.131 C/V), 2.886V (-0.973 C/V), and 3.193V (-1.462 C/V), reflecting changes in reaction kinetics and resistance build-up. The gradual decrease in peak intensity at higher voltages, such as 4.114V (-0.259 C/V) and 3.711V (-0.140 C/V), suggests a decline in lithium-ion availability and a reduction in active electrode sites over time.

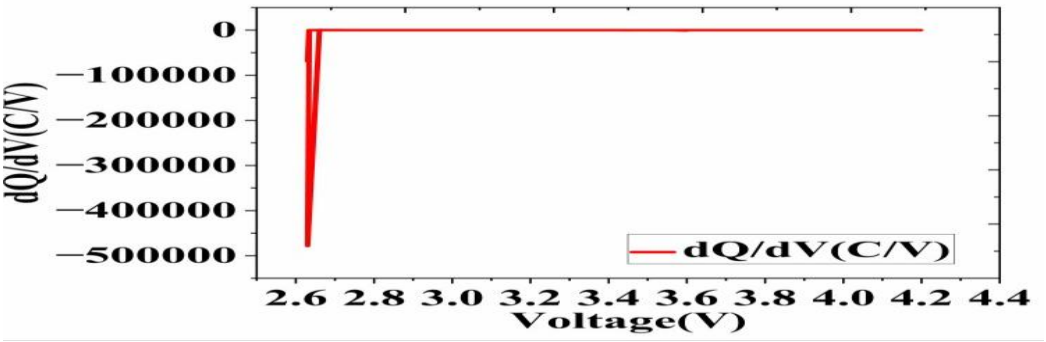

Fig. 3.21: dQ/dV (Differential Capacity) vs. Voltage (Volts) of Li-NCM Ce

4.5.2Aging Characteristics from Peak Analysis in Dq/Dv:

With continuous cycling, the shifting and diminishing of differential capacity peaks indicate electrode degradation, solid electrolyte interphase (SEI) layer growth, and loss of active material. Notable peak shifts around 3.863V (-0.089 C/V) and 2.941V (-0.394 C/V) suggest lithium-ion trapping and electrolyte instability. Peak broadening and reduction at 3.772V (- 0.015 C/V) and 3.627V (-0.021 C/V) indicate increased internal resistance and polarization effects. The pronounced negative peaks at 2.652V (-2.244 C/V) and 2.634V (-2.131 C/V) point to rising impedance due to side reactions and electrode degradation. These observations confirm capacity fade, lithium diffusion limitations, and increased resistance, all of which are key indicators of aging in Li-NCM cells.

CONCLUSION

Based on the experimental investigation, the LFP cell exhibits stable electrochemical performance, maintaining a steady capacity of roughly 2.6 Ah during numerous cycles of charge and discharge. Cell temperatures increased from 25°C to a peak of 56.45°C (average ≈ 39°C) according to thermal assessments, indicating efficient internal heat dissipation. However, when temperatures surpass 45.95°C in high-power applications, further cooling may be required. The dependability of voltage-based SOC estimate techniques is supported by the linear relationship between open-circuit voltage (OCV) and state of charge (SOC). The broadening and attenuation of differential capacity (dQ/dV) peaks, which show increasing internal resistance, the formation of the solid electrolyte interphase (SEI) layer, and progressive loss of active material, are further signs of aging. Together, our results demonstrate the resilience and degradation characteristics of LFP cells, providing important information for battery management and lifecycle forecasting.

REFERENCES

1. Britala, L., Marinaro, M. and Kucinskis, G., 2023. A review of the degradation mechanisms of NCM cathodes and corresponding mitigation strategies. *Journal of Energy Storage*, X, pp.1–25.
2. Brosa Planella, F., Ai, W., Boyce, A.M., et al., 2022. A continuum of physics-based lithium-ion battery models reviewed. *Journal of Power Sources*, 529, p.231359.
3. Goli, P., Legedza, S., Dhar, A., et al., 2013. Graphene-enhanced hybrid phase-change materials for thermal management of Li-ion batteries. *Nano Letters*, 13, pp.6152–6159.
4. Biju, N. and Fang, H., 2022. BattX: An equivalent circuit model for lithium-ion batteries over broad current ranges. *Journal of Energy Storage*, 58, p.106459.
5. Zhang, R. and Pan, Z., 2019. Model identification of lithium-ion batteries considering current-rate effects on battery impedance. *Proceedings of ICPRE*, pp.305–309.
6. Ramadass, P., Haran, B., White, R. and Popov, B.N., 2003. Mathematical modeling of the capacity fade of Li-ion cells. *Journal of Power Sources*, 123, pp.230–240.
7. Kim, D.H., et al., 2018. Critical review on battery state of charge estimation methods for electric vehicles. *IEEE Access*, 6, pp.1832–1843.
8. Zhang, S., Guo, X., et al., 2020. Data-driven Coulomb counting method for state of charge calibration and estimation. *Sustainable Energy Technologies and Assessments*, 37, pp.100–110.
9. Xiong, R., Cao, J., Yu, Q., et al., 2018. Critical review on battery State of Charge estimation methods for electric vehicles. *IEEE Access*, 6, pp.1832–1843.

10. Steinhardt, D., Bui, T.N., et al., 2023. Influence of Li-ion battery ECM parameter dependencies on predicted heat generation in real-life drive cycles. *Batteries*, 9(5), p.274.
11. Lin, X., Kim, Y., Mohan, S., Siegel, J. and Stefanopoulou, A.G., 2019. Modeling and estimation for advanced battery management. *Annual Review of Control, Robotics, and Autonomous Systems*, 2, pp.1–23.
12. Hui, X. and Peng, H., 2024. Comparative research on RC equivalent circuit models for Li-ion batteries in EVs. *Applied Sciences*, 14, p.10876.
13. Li, S., Bhadriraju, B., et al., YYYY. Deep neural network aging estimation with high-fidelity SPM models. *Journal of Energy Storage*, X, pp.100–112.
14. Li, T.K.D., et al., 2011. Dynamic modeling of Li-ion batteries using equivalent electrical circuit. *Journal of the Electrochemical Society*, 158(8), pp.A755–A763.
15. Sivasamy, S., Sundaramoorthy, P., & Beno, M. (2023). A comprehensive investigation of outer rotor permanent magnet switched reluctance motor for enhanced performance in electric vehicles. *Canadian Journal of Electrical and Computer Engineering*, 46(4), 342–347.
16. Prabhu S, Vinod S, Rudhra S, Balaji M, 2025. Green Evaluation of Lithium Iron Phoshate(LPF) Batteries: Enviromental Consequences of Electrochemical, Thermal and Aging Factor. International Journal of Environmental Sciences, Vol.11 No. 3, pp.957-971.
17. Saravanan Sivasamy, Vinod S, Balaji M, Rudhra S, Prabhu, 2025. Electrochemical and Thermal Characterization of the Li-NCM NM3100 Cell for EV Applications. . International Journal of Environmental Sciences, Vol.11 No. 4, pp.947-961.
18. Madhaiyan, V., Murugesan, R., Sengottaiyan, S., Muniyan, V., Vijayakumar, A., & Sundaramoorthy, P. (2023). Analysis of performance for multilevel inverters utilizing different pulse width modulation techniques. *Proceedings of the 1st Int. Conf. on Advances in Electrical, Electronics and Computational Intelligence (ICAEECI)*, Tiruchengode, India, 1–7.
19. Arun, V. & Prabhu, S. (2022). Design and vibration analysis on EMS by using Block Lanczos method for humanoid robotics arm applications. *International Journal on Interactive Design and Manufacturing (IJIDeM)*.
20. Prabhu, S., Balaji, M., & Kamaraj, V. (2015). Analysis of two phase switched reluctance motor with flux reversal free stator. *2015 IEEE 11th International Conference on Power Electronics and Drive Systems (PEDS)*, Sydney, Australia, 320–325.
21. Sundaramoorthy, P., Vijayakumar, A., Rajkumar, K., Ponnusamy, J., Chandrasekaran, G., & Madhaiyan, V. (2024). Impacts of laminating core materials on permanent magnet synchronous motor by Newton–Raphson method. *IEEE Canadian Journal of Electrical and Computer Engineering*, 47(2), 105–110.
22. Sundaramoorthy, P. & Mahadevan, B. (2018). Analysis and implementation of two phase flux reversal free doubly salient machine. *Journal of Magnetics*, 23(3), 350–359.
23. Prabhu, S., Arun, V., Balaji, M., Kalaimagal, V., Manikandan, A., & Reddy, B.M. (2023). Investigations on brushless DC motors for automotive systems. *9th International Conference on Electrical Energy Systems (ICEES)*, Chennai, India, 138–142.
24. Likhitha, K., Hitaishi, M., Arshad, K., Arun, V., Prabhu, S., & Shanathi, B. (2023). Modular seven level inverter (M7LI) with level shifted variable frequency control. *9th International Conference on Electrical Energy Systems (ICEES)*, Chennai, India, 509–513.
25. Prabhu, S., Arun, V., Balaji, M., Kalaimagal, V., Manikandan, A., & Chandrasekar, V. (2023). Electromagnetic analysis on brushless DC hub motor for electrified transportation systems. *9th International Conference on Electrical Energy Systems (ICEES)*, Chennai, India, 179–183.
26. Prabhu, S., Arun, V., Balaji, M., Kalaimagal, V., Manikandan, A., & Chandrasekar, V. (2023). Finite element analysis on interior permanent magnet machine for propulsion system. *International Conference on Power, Instrumentation, Energy and Control (PIECON)*, Aligarh, India, 1–5.
27. Vinod, S., Balaji, M., & Prabhakar, M. (2015). Robust control of parallel buck fed buck converter using hybrid fuzzy PI controller. *IEEE 11th International Conference on Power Electronics and Drive Systems (PEDS)*, Sydney, Australia, 347–351.
28. Vinod, S., Navin, V., & Sivaraj, C. (2011). Simulation of power electronics-based controller for grid connected wind turbine. *International Conference on Emerging Trends in Electrical and Computer Technology (ICETECT)*, Nagercoil, India, 255–260.
29. Satish Kumar, S., Pramila, V., Rudhra, S., Vinod, S., & Lakshmi, D. (2025). Enhancing demand response and energy management in multi-microgrid systems with renewable energy sources. *Renewable Energy*, 253, 123490.
30. Vinod, S., Balaji, M., Rudhra, S., & Prabhu, S. (2023). Solar powered DC arc welding machine – An initiative towards efficient and sustainable energy. *Journal of Environmental Protection and Ecology*, 24(3), 888–894.
31. Vinod, S., Rudhra, S., Prakash, J.A., & Kumar, M.J. (2022). Implementation of eco-friendly automatic seed sowing machine. *International Conference on Computer, Power and Communications (ICCPC)*, Chennai, India, 527–530.
32. Vinod, S. & Balaji, M. (2020). Variable speed PMSG design and implementation for wind driven welding power source. *Circuit World*, 46(3), 161–167.